


RESEARCH ARTICLE

Process Sensing and Control

Impact of different trace elements on metabolic routes during heterotrophic growth of *C. ljungdahlii* investigated through online measurement of the carbon dioxide transfer rate

Marcel Mann¹  | Darina Effert¹ | Patrick Kottenhahn^{1,2} | Aline Hüser¹ | Gabriele Philipps² | Stefan Jennewein² | Jochen Büchs¹

¹AVT – Biochemical Engineering, RWTH Aachen University, Aachen, Germany

²Department for Industrial Biotechnology, Fraunhofer Institute for Molecular Biology and Applied Ecology IME, Aachen, Germany

Correspondence

Jochen Büchs, AVT – Biochemical Engineering, RWTH Aachen University, Forckenbeckstraße 51, 52074 Aachen, Germany.
Email: jochen.buechs@avt.rwth-aachen.de

Funding information

Funded by the German Federal Ministry of Education and Research (BMBF), Grant Number: 03INT513BE as well as the European Union. This project has received funding from the European Union's Horizon 2020 Research and Innovation Programme under Grant Agreement No. 761042 (BIOCON-CO₂). This output reflects the views only of the author(s), and the European Union cannot be held responsible for any use which may be made of the information contained therein.

Abstract

Synthesis gas fermentation using acetogenic clostridia is a rapidly increasing research area. It offers the possibility to produce platform chemicals from sustainable C1 carbon sources. The Wood-Ljungdahl pathway (WLP), which allows acetogens to grow autotrophically, is also active during heterotrophic growth. It acts as an electron sink and allows for the utilization of a wide variety of soluble substrates and increases ATP yields during heterotrophic growth. While glycolysis leads to CO₂ evolution, WLP activity results in CO₂ fixation. Thus, a reduction of net CO₂ emissions during growth with sugars is an indicator of WLP activity. To study the effect of trace elements and ventilation rates on the interaction between glycolysis and the WLP, the model acetogen *Clostridium ljungdahlii* was cultivated in YTF medium, a complex medium generally employed for heterotrophic growth, with fructose as growth substrate. The recently reported anaRAMOS device was used for online measurement of metabolic activity, in form of CO₂ evolution. The addition of multiple trace elements (iron, cobalt, manganese, zinc, nickel, copper, selenium, and tungsten) was tested, to study the interaction between glycolysis and the Wood Ljungdahl pathway. While the addition of iron(II) increased growth rates and ethanol production, added nickel(II) increased WLP activity and acetate formation, reducing net CO₂ production by 28%. Also, higher CO₂ availability through reduced volumetric gas flow resulted in 25% reduction of CO₂ evolution. These online metabolic data demonstrate that the anaRAMOS is a valuable tool in the investigation of metabolic responses i.e. to determine nutrient requirements that results in reduced CO₂ production. Thereby the media composition can be optimized depending on the specific goal.

KEYWORDS

anaRAMOS, *Clostridium ljungdahlii*, online measurement, syngas, trace elements

This is an open access article under the terms of the [Creative Commons Attribution](https://creativecommons.org/licenses/by/4.0/) License, which permits use, distribution and reproduction in any medium, provided the original work is properly cited.

© 2022 The Authors. *Biotechnology Progress* published by Wiley Periodicals LLC on behalf of American Institute of Chemical Engineers.

1 | INTRODUCTION

The climate goals defined by the European commission demand a drastic reduction of greenhouse gas emission with two targets set for 2030 and 2050, requiring new technological advances.^{1,2} Several strategies of “carbon capture and storage” and “carbon capture and utilization” are under investigation. One promising technology for future applications is gas fermentation. Gaseous carbon and energy sources from industrial exhaust gas or gasified organic materials like municipal waste or lignocellulosic biomass can be used as a feedstock to produce platform chemicals and fuels.^{3–6} These gases have in common that they are composed of H₂, CO₂, and CO in differing ratios and are called synthesis gas or syngas. As a group generally referred to as acetogens, several bacterial species can use these gases as a substrate for growth and production of a wide array of industrially relevant chemicals, especially organic acids and alcohols.^{7–11} Acetogens employ a linear carbon fixation pathway called the Wood-Ljungdahl pathway (WLP), yielding acetyl-CoA as an energy rich intermediate^{12,13} (shown in Figure 1). The ability to capture carbon from industrial or agricultural byproducts turns these microorganisms into promising biocatalysts, to reduce our global carbon footprint through sustainable production of commodity chemicals.

Even though acetogenic bacteria are generally investigated concerning their ability to grow autotrophically and turn syngas into commodity chemicals, carbohydrates as a carbon source provides an easily accessible substrate that is neither toxic nor limited by gas-water transfer rates. While consumption of C₆ sugars such as glucose or fructose leads to the emission of CO₂ in various anaerobically grown organisms, acetogens can convert fructose stoichiometrically into three molecules of acetate without net production of CO₂ by using the same metabolic route as used for autotrophic growth.¹⁴ This is achieved by employing the WLP to reduce the CO₂ evolved during glycolysis with the electrons derived from the sugar. The formation of three moles of acetate per mole of fructose was reported early in the research of acetogens, when the second isolated acetogen, *Clostridium thermoaceticum*, was described in 1942.^{15,16} Employing the WLP as a metabolic module to reestablish redox homeostasis during growth on fructose allows acetogens to conserve more energy than their competitors in the same environment, providing them with an evolutionary edge.^{17,18} Furthermore, the WLP has been shown to allow acetogens to access growth substrates like lactate¹⁹ or ethanol,^{20–22} which are products of many anaerobic fermentations. Both compounds are relatively common in anaerobic environments and inaccessible as carbon and sources for many other organisms. It has been demonstrated for the model acetogen *C. ljungdahlii*, that the genes of the WLP pathway are constitutively transcribed. When grown on CO/CO₂ + H₂, where the WLP acts as the key metabolic route, transcription of the WLP genes is only increased 1.31–2.06 fold compared to growth with fructose, where the WLP provides a supporting role for the hexose metabolism^{23,24} (Figure 1).

During glycolysis, fructose is converted into two coenzymeA-bound acetyl-groups, two molecules of CO₂, and eight electrons.

Electrons are carried by four redox equivalents, namely two NADH and two reduced ferredoxin. Both CO₂ molecules can then dependent on the activity of the WLP, be reduced with electrons from the redox equivalents and incorporated into one additional acetyl-CoA via the WLP.¹⁴ This remarkable feature allows for reestablishing the redox homeostasis and conserves additional energy, if acetate is produced from the acetyl-CoA. Thus, acetogens are able to conserve more energy during growth on fructose, compared to organisms without the WLP, which produce, for example, ethanol + CO₂ or lactate from sugars.¹⁷ If fructose is the only available electron donor, redox homeostasis allows for the formation of three molecules of acetate from fructose. However, at low CO₂ availability due to excessive stripping into the gas phase or in the presence of additional gaseous electron donors like H₂ or CO, a shift from CO₂ reduction toward reduction of acetate to ethanol allows the cells to conserve more energy per carbon. This in turn leads to net CO₂ emission instead of strict homoacetogenesis. During autotrophic growth with H₂ as electron source, acetogens employ a bifurcating hydrogenase to transfer the electrons from H₂ to NAD(P)H and Fd.^{14,25} In theory, during growth with fructose, this enzyme might act in reverse and lead to the production of traces of H₂. *Moorella thermoacetica* for example, is known to produce small traces of H₂ during growth with glucose (2 mmol H₂ per 100 mmol glucose) under CO₂ limitation.²⁶ This, however, might be neglected for the purpose of this study, since this amount of H₂ evolution only accounts for a small fraction of the electrons transferred during the glycolysis. Since eight electrons per hexose are transferred to electron carriers during glycolysis, 100 mM glucose provide 800 mM of electrons. Since two electrons are needed for the production of a H₂ molecule, the electrons derived from 100 mM of glucose would in theory allow for the production of 400 mM of hydrogen. Thus, the observed 2 mmol of H₂ produced from 100 mmol of glucose by *M. thermoacetica* only constitute 0.5% of the available electrons in the cited study. Hence, the interaction and activity of these pathways, glycolysis, WLP and reduction of acids to alcohols, determine carbon conversion efficiency and product ratios.

Due to the increased industrial value and the broader field of applications of alcohols compared to organic acids, research generally focuses on increasing yield and selectivity for alcohol production.^{27–33} Various methods to genetically increase the spectrum of available products and to improve specificity for the targeted product have been reported.^{34–36} Another route for higher selectivity and improved titers of targeted products is the optimization of fermentation conditions, especially media composition. Variation of the gas composition and gas availability has also been reported to influence the product ratio of acetate to ethanol. For example, an increased CO availability resulted in higher alcohol and decreased acid production.^{14,25,26}

An essential issue in alcohol production is the availability of necessary cofactors for enzymes involved in the required pathways. Since many enzymes in acetogens depend on metallic cofactors³⁷ (Figure 1), optimization of trace element compositions is crucial for optimal enzyme activity in syngas fermentation. The metal involved in the most significant number of metabolic conversions in acetogens

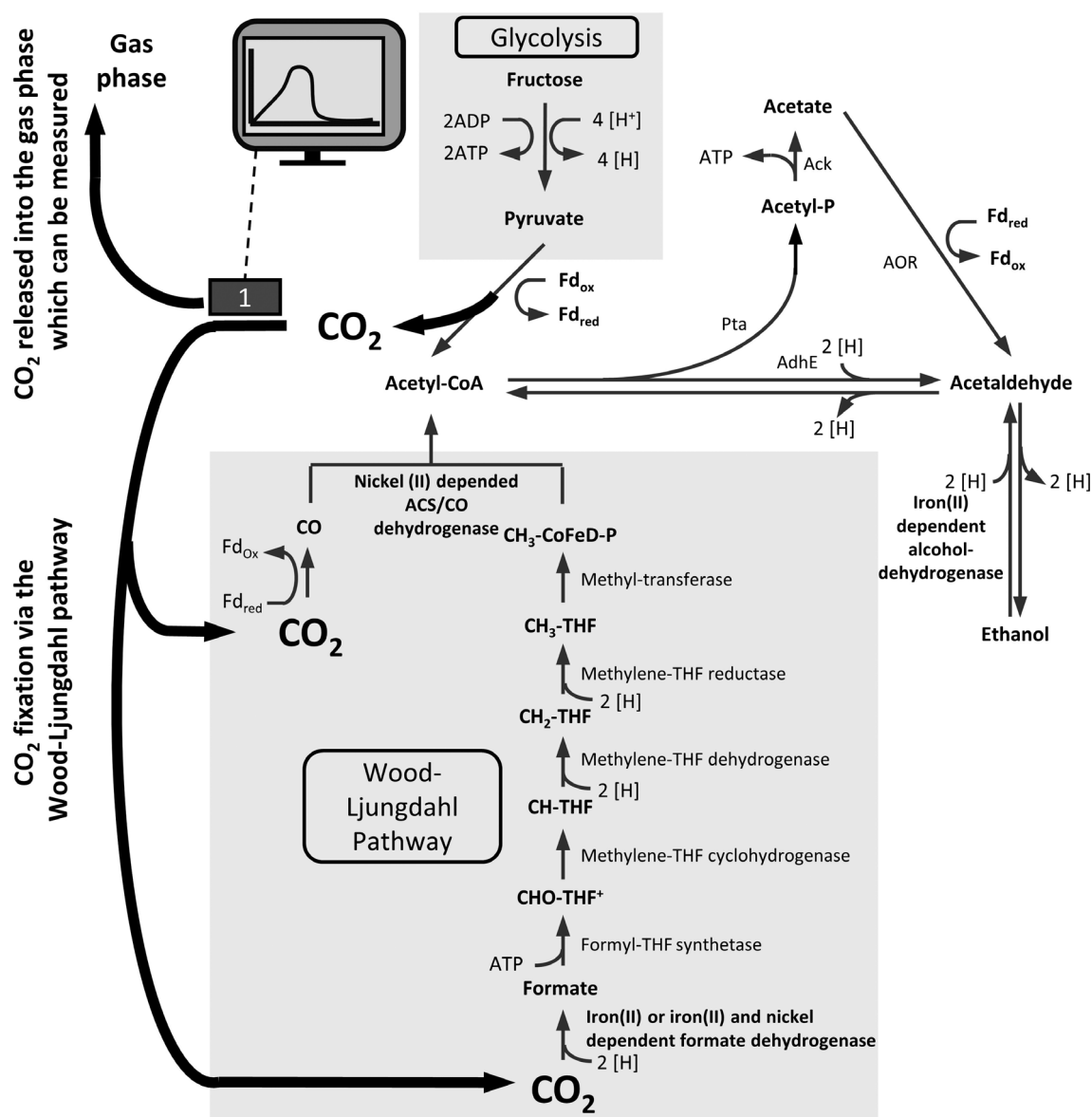


FIGURE 1 Carbon and electron flux during growth on fructose of *C. ljungdahlii* with online CTR measurement using the anaRAMOS. CO_2 evolved during glycolysis can be fixed in the Wood-Ljungdahl pathway or it can be exhausted into the gas phase. Exhausted carbon dioxide is detected by the anaRAMOS (1). For detailed explanation please see main text. Ack: acetate kinase, ACS/CODH: bifunctional acetyl-CoA synthase/CO dehydrogenase, AdhE: bifunctional aldehyde–/alcohol dehydrogenase, AOR: aldehyde-ferredoxin oxidoreductase, PFOR: pyruvate-ferredoxin oxidoreductase, pta: phosphotransacetylase. If the electron carriers NADH or ferredoxin are involved in reactions, only the reduced form of the electron carrier is shown for easier readability of the figure. For the same reason, free CoA, THF and $ADP + Pi$ were omitted. $[H]$ is used as a placeholder for electron carriers (proton + electron), if the electron carrier involved in the reaction is variable. Possible electron transfer between molecular hydrogen, NADH and ferredoxin via bifurcating hydrogenase and rnf complex are not shown. Products are not stoichiometric, as dependent on multiple parameters. Source: Figure modified from Köpke et al.¹³

is iron(II).³⁸ It is required in the electron carrier ferredoxin,^{39,40} in many enzymes catalyzing reactions of the WLP³⁷ and alcohol dehydrogenases and aldehyde oxidoreductases^{13,41} (Figure 1). Additionally, it was found to be required in concentrations an order of magnitude higher than almost all other trace elements in an optimized trace element solution for alcohol production in *C. carboxidivorans*.⁴² But also other metals like nickel, selenium, tungsten, zinc, and cobalt are essential,^{31,42,43} due to their involvement in several reactions.

In the first step of the WLP and the reduction of necessary electron carriers, iron(II) and nickel(II) are essential. The genome of the model acetogen *C. ljungdahlii* encodes four [FeFe] hydrogenases and one [NiFe] hydrogenase. These hydrogenases are either involved in reducing electron carriers like NAD(P)H, and ferredoxin (containing FeS-cluster) with electrons derived from H_2 or are part of the enzyme complex catalyzing the initial step of the WLP, reduction of CO_2 to formate.¹⁴ Both metals are also essential for several further reactions

in the WLP, like the final fusion of both reduced C1 intermediates to the coenzymeA-bound acetyl-group by the CO-dehydrogenase/acetyl-CoA-synthase (CODH/ACS)¹³ (Figure 1). In this final reaction of the WLP, a cobalamin corrinoid iron(II)-sulfur protein is essential for transferring the methyl group from THF to form acetyl-CoA.^{37,44}

From here on, two distinct routes are possible. Either acetyl-CoA is directly reduced to ethanol via acetaldehyde by an iron(II)-dependent bifunctional alcohol-/aldehydedehydrogenase (adhE), with electrons derived from two NADH, or acetate is produced first by phosphotransacetylase and acetate kinase, leading to the formation of one ATP (Figure 1). Acetate can then be further reduced to acetaldehyde via a tungsten-dependent aldehyde-ferredoxin-oxidoreductase (aor) with electrons derived from ferredoxin. Finally, ethanol is produced in a second step from acetaldehyde via adhE.⁴¹ Even though the discussed number of enzymes involved in the WLP requiring metals as cofactors is not comprehensive, it clearly emphasizes the need for sufficient trace metal availability in the fermentation medium. Different studies investigated trace element composition and showed the inherent potential in fermentation optimization by adjusting the trace element composition.^{31,42,43} YTF medium is a medium commonly employed for heterotrophic growth of *C. ljungdahlii*.^{36,45–49} Since YTF (Yeast extract-Tryptone-Fructose) medium only contains the trace elements provided through yeast extract and tryptone, it is debatable whether all required trace elements for the maximum activity of the WLP are provided in this medium.

To study the impact of trace metals on metabolic activity, the anaerobic Respiration Activity Monitoring System (anaRAMOS) device was used. The anaRAMOS offers the possibility of real-time online monitoring of the carbon dioxide transfer rate (CTR) in up to eight parallel shake flasks.^{49,50} The measured CTR is a direct quantitative indication of metabolic activity and can be used to calculate the total amount of produced net CO₂ (CT). As already discussed, in hexose metabolism, acetogens first produce two mol CO₂ per sugar, which can subsequently be reduced to acetyl-CoA in the WLP with electron carriers reduced during glycolysis. Any relative reduction of the observed CO₂ production by the anaRAMOS is an indicator of the WLP activity. This is the case, because in all experiments fructose was fully consumed. Hence, the carbon converted into biomass, acetate and ethanol was the same in all experiments.

The anaRAMOS has previously been demonstrated to be a helpful tool to optimize growth conditions.⁴⁹ Through this method an iron(II)-deficiency in YTF medium for *C. ljungdahlii* was detected. A model was introduced, which allows determination of the necessary amount of iron(II) for unlimited growth on a given amount of fructose.⁴⁹ In the present study, the addition of metal salts from PETC 1754 medium (iron, cobalt, manganese, zinc, nickel, copper, selenium, and tungsten) to YTF medium was analyzed to demonstrate the influence of different trace elements on the cultivation of *C. ljungdahlii* in complex medium. For this goal the anaRAMOS was deployed to monitor changes in metabolic activity through online measurement of CO₂ evolution. These results highlight the benefit of the anaRAMOS in understanding microbial metabolism. Additionally, due to semi-

continuous ventilation, the anaRAMOS is closer to industrial fermentation conditions, compared to non-ventilated, but commonly used serum bottles. A special focus is set on the interaction of glycolysis and WLP. This is done by evaluating the CO₂ production, dependent on the experimental setting.

2 | MATERIAL AND METHODS

2.1 | Strain and media

Clostridium ljungdahlii (DSMZ 13528) was obtained from the Deutsche Sammlung von Mikroorganismen und Zellkulturen (DSMZ, Braunschweig, Germany). YTF medium, as previously reported, was used for all cultivations.⁵¹ The growth medium consisted of the main stock solution, fructose stock solution, and cysteine stock solution. The 1.5 fold concentrated main stock solution contained per liter 15 g yeast extract (Yeast extract, Oxoid™, France), 24 g tryptone (Tryptone from Casein pancreatic digested, CarlRoth, Germany), 6 g NaCl (CarlRoth, Germany) and was autoclaved. The 20 fold concentrated fructose stock solution contained per liter 100 g fructose (CarlRoth, Germany) and was autoclaved. L-Cysteine (Sigma-Aldrich, Germany) stock solution was concentrated 10 fold and contained per liter 7.5 g L⁻¹ cysteine-HCl and was sterile filtered. Right after, the stock solution was made anoxic by purging with 100% N₂. Trace element solution (TE) or single trace elements were added to the experiments when indicated (amounts are given for each experiment). The composition of the TE solution was derived from ATCC medium 1754 PETC trace elements components containing per liter 0.8 g (NH₄)₂Fe(SO₄)₂·6H₂O, 0.2 g CoCl₂·6H₂O, 1 g MnSO₄·H₂O, 0.02 g Na₂MoO₄·2H₂O, 0.0002 g ZnSO₄·7H₂O, 0.02 g NiCl₂·6H₂O, 0.02 g CuCl₂·2H₂O, 0.02 g Na₂SeO₃·5H₂O, 0.02 g Na₂WO₄·2H₂O and 2 g nitrilotriacetic acid. Single trace element solutions were prepared to contain per liter 0.2 g CoCl₂·6H₂O, 0.8 g (NH₄)₂Fe(SO₄)₂·6H₂O or 0.02 g NiCl₂·6H₂O, respectively. The TE solution and single trace elements were sterile filtered.

Before each experiment, the main stock solution, fructose stock solution, and cysteine stock solution were mixed. Trace element solution or single trace elements were added according to the experiment's aim (details are given for each experiment). The pH was set to a value of 6 with HCl, and the final volume was adjusted using sterile deionized water. The completed medium was transferred into serum bottles or shake flasks under sterile conditions. Serum bottles were flushed for 20 min before inoculation using 90% ultra-high purity (99.999%) nitrogen (Praxair, Germany) and 10% carbon dioxide (99.995%) (Praxair, Germany). For anaRAMOS cultivations, the shake flasks containing aerobic medium were installed in the anaRAMOS device and flushed for a minimum of 2 h using ultra-high purity (99.999%) nitrogen (Praxair, Germany), while constant shaking at 100 min⁻¹ (*d*₀ = 5 cm). Prior to each experiment, a pressure test was performed in order to verify tightness of each cultivation flask. Hence, oxygen contamination can be excluded as all flasks were air tight. Cryo stocks of cells were stored at -80°C after the addition of 10%

anoxic DMSO to an actively growing culture in YTF medium at $OD_{600} = 0.8$.

2.2 | Cultivation conditions

Two sequential pre-cultures were grown in serum bottles at 37°C and a shaking frequency of 220 min⁻¹ at a shaking diameter of $d_0 = 3$ mm. The first pre-culture with a total filling volume of 10 ml (in 100 ml serum bottles) was inoculated with a thawed cryo stock in a ratio of 1:10. After 24 h, the second pre-culture with a filling volume of 50 ml (in 250 ml serum bottles) was inoculated in a 1:10 ratio. After 20–24 h, an optical density of 1.0 was reached, and the second pre-culture was used to inoculate the main culture. Main cultures were inoculated in a 1:10 ratio unless stated differently. The pre-culture was transferred into the RAMOS flasks through a septum using a 5 ml syringe with a cannula.

All main cultivations were performed in non-baffled 250 ml shake flasks at 37°C in an orbital climo-shaker ISFX-1 from Kühner AG (Switzerland). An in-house built anaRAMOS device was used for semi-continuous online monitoring of the CTR.⁵⁰ A filling volume (V_L) of 50 ml was used at a shaking diameter (d_s) of 50 mm and a shaking frequency (n) of 100 min⁻¹. Each shake flask was ventilated using ultra-high-purity (99.999%) nitrogen (Praxair, Germany) at a flow rate of 5 ml min⁻¹ per shake flask (flow phase). A detailed setup of the anaRAMOS device and calculation of the CTR is reported in previous publications,^{49,50} as well as in the Supplementary Information S1 and Figure S1.

2.3 | Offline analysis

For offline analysis, shake flasks were removed from the anaRAMOS after the cultivation was terminated. The optical density (OD) was measured, after adequate dilution (OD 0.1–0.3), at a wavelength of 600 nm using a Genesys 20 Photospectrometer (ThermoScientific, USA). Subsequently, the OD was used to calculate the cell dry weight. For this, the OD to cell dry weight (CDW) correlation was determined as shown in Figure S2. Equation (1) was used for calculation. For CDW measurement a pre-dried and pre-weight filter paper was used. Ten-milliliter samples were transferred onto the filter paper while vacuum was applied. Filter papers were dried for 48 h and the weight was taken thereafter.

$$OD = 0.0019 \cdot CDW \left[\frac{g}{L} \right] \quad (1)$$

Biomass composition of $CH_{1.666}N_{0.23}O_{0.27}$ with a molecular weight of 20.7 g mol⁻¹ was used to calculate the carbon content in biomass.⁵² Two milliliters of sample were centrifuged for 5 min at RCF = 18,000 g (Rotina 35 R, Hettich Zentrifugen, Germany). The supernatant was partly used for pH measurement (HI221 Microprocessor pH Meter, Hanna Instruments, Germany). The remaining

supernatant was stored at –20°C for High-Performance Liquid Chromatography (HPLC) analysis. For HPLC analysis, samples were thawed, filtered (pore size 0.2 μm), and stored at 4°C until analysis. HPLC analysis (Prominence HPLC, Shimadzu, Germany) was performed using an organic acid column (ROA-Organic Acid H+, Phenomenex Inc., Germany) at 60°C and 5 mM H₂SO₄ as the mobile phase with a flow rate of 0.8 ml min⁻¹. Elution was detected using a Refracting Index Detector (RID-10A, Shimadzu, Germany).

3 | RESULTS AND DISCUSSION

3.1 | Influence of the addition of trace elements (TE) on *C. ljungdahlii* metabolic activity

The first goal of this work was to gain insights into the influence of added trace elements (TE) on the chemotrophic cultivation of *C. ljungdahlii*. Therefore, cultivations on standard YTF medium and YTF medium supplemented with 10 ml L⁻¹ trace element solution from PETC 1754 medium were performed, and the CTR was measured with the anaRAMOS device (Figure 2). Cultivation on standard YTF medium resulted in two CTR peaks (Figure 2a). Phase I (until peak I) was mainly based on consumption of complex media components, while phase II was mainly based on fructose conversion, as already reported in a previous study.⁴⁹ For a better overview, Phases and Peaks are also outlined in Figure S3. Supplementation with TE resulted in a shortening of phase I from 12 to 11 h compared to the reference without added TE. The maximum CTR of the first peak (at the end of phase I) was, on average, 1.3 mmol L⁻¹ h⁻¹ for both cultivations. The cultivation duration until fructose depletion with supplemented TE was reduced by 42.5% from 40 to 23 h compared to the reference. Fructose depletion is indicated by the drop of the CTR to 0 mmol L⁻¹ h⁻¹ at about 50 h. A reference experiment with offline data is shown in Figure S4. The second CTR peak (during phase II) of the cultivation with TE reached a maximum CTR of 3.2 mmol L⁻¹ h⁻¹, while in standard YTF medium, the maximum CTR was only 2.1 mmol L⁻¹ h⁻¹. In comparison, the cultivation without TE displayed a plateau after the second CTR peak for the remainder of phase II. In the cultivation with added TE, the CTR decreased sharply after the CTR peak at 19 h and reached 0 mmol L⁻¹ h⁻¹ after 23 h of cell growth. The progression of the CTR over time for the cultivation with TE did not adhere to the typical CTR curve shape expected for unlimited growth.⁵³ Reasons for this were investigated in the subsequent experiments reported in this manuscript.

To calculate the total CO₂ production throughout the cultivation, the CTR curve can be integrated to obtain the CT value (Figure 2b). Providing 5 g L⁻¹ (27.8 mmol L⁻¹ = 166.8 mmol L⁻¹ carbon) of fructose results in a theoretical CT of 55.6 mmol L⁻¹ CO₂, if the WLP is inactive (two mole of CO₂ are formed per mole of fructose, as shown in Figure 1). CO₂ utilized via the WLP is not released into the gas phase and can thus not be detected by the anaRAMOS device. Therefore, a reduction of the observed CT compared to a reference cultivation is an indicator for increased carbon fixation in the WLP. In our

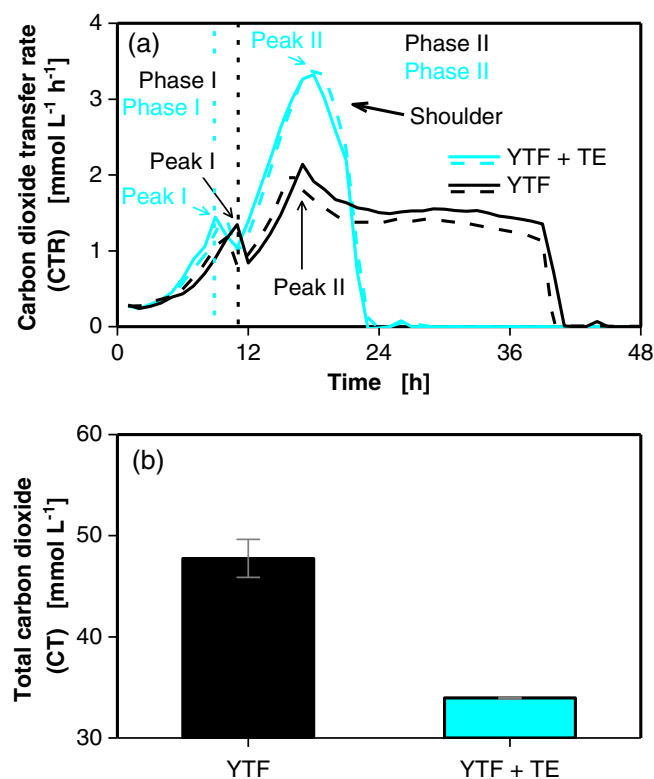


FIGURE 2 Metabolic activity of *C. ljungdahliae* grown in complex medium with fructose in the absence (YTF) and in the presence (YTF + TE) of added trace elements (as described in material and methods section) monitored by the anaRAMOS. Each condition was tested in duplicates (dashed lines). (a) Carbon dioxide transfer rate (CTR) ($\text{mmol L}^{-1} \text{h}^{-1}$). (b) Total carbon dioxide (CT) (mmol L^{-1}) calculated as integral from the online CTR measurement (Phase I + II). Error bars indicating minimal and maximal value. Cultivation conditions: Temperature: $T = 37^\circ\text{C}$, $\text{pH}_{t0} = 6$, shaking frequency: $n = 100 \text{ min}^{-1}$, shaking diameter: $d_o = 50 \text{ mm}$, culture volume: $V_L = 50 \text{ ml}$, absolute gas flow rate: $5 \text{ ml min}^{-1} \text{ N}_2$, medium = YTF medium, initial fructose concentration $c_{t0} = 5 \text{ g L}^{-1}$, inoculation density: $\text{OD}_{t0} = 0.1$.

experiment, standard YTF medium resulted in a CT of 48 mmol L^{-1} (Figure 2b), indicating only background WLP activity. The slightly reduced amount of total detected CO_2 , compared to the theoretical yield from fructose (55.6 mmol L^{-1}), could also be caused by medium dilution during inoculation. In cultures with added TE solution, the CT was reduced to 35 mmol L^{-1} . The change of CT indicates initiation of WLP activity in the presence of added TE, since CO_2 produced from fructose can only either be utilized via the WLP or exhausted. These first results demonstrate that even when grown in the well-established YTF medium, metal availability limits metabolic activity of *C. ljungdahliae*, which can be alleviated by supplementing additional trace elements.

To examine, which TE influences the cultivation need further analysis, all trace elements were added individually (Figure 3). Distinct changes in CTR progression were only observed with iron(II) and cobalt(II) (Figure 3a). The addition of iron(II) led to a 13% increase in CT compared to the reference without added TE (Figure 3b),

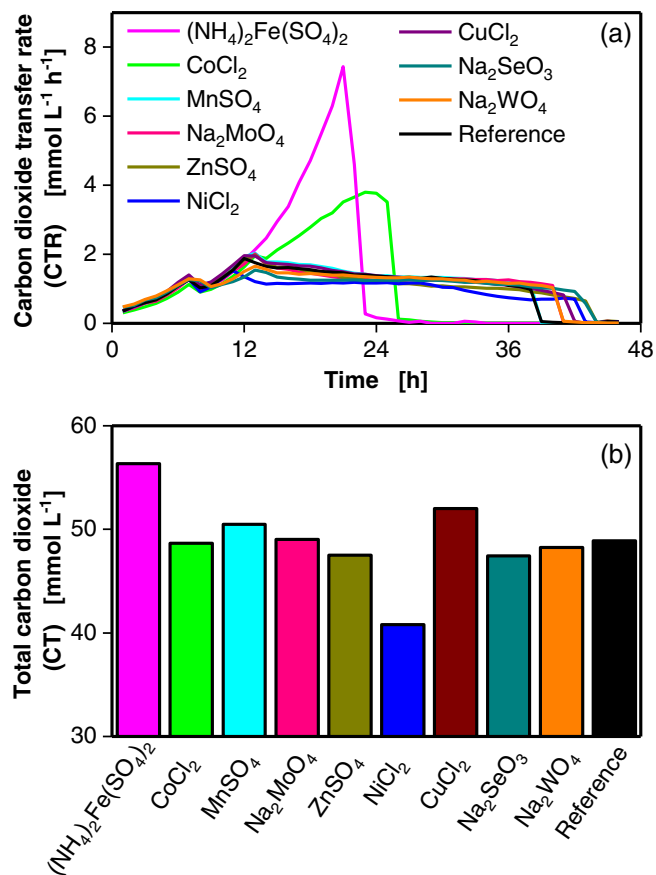


FIGURE 3 Influence of addition of different trace elements on batch cultivation of *C. ljungdahliae* (DSM 13528) in YTF medium on fructose in ten 250 ml anaRAMOS flasks (two experiments). Reference YTF medium without added TE, or with supplemented 8 mg L^{-1} Ammonium iron(II) sulphate hexahydrate ($(\text{NH}_4)_2\text{Fe}(\text{SO}_4)_2 \cdot 6\text{H}_2\text{O}$), 2 mg L^{-1} Cobalt(II) chloride hexahydrate ($\text{CoCl}_2 \cdot 6\text{H}_2\text{O}$), 10 mg L^{-1} Manganese sulphate monohydrate ($\text{MnSO}_4 \cdot \text{H}_2\text{O}$), 2 mg L^{-1} Sodium molybdate dihydrate ($\text{Na}_2\text{MoO}_4 \cdot 2\text{H}_2\text{O}$), 0.002 mg L^{-1} Zinc sulphate heptahydrate ($\text{ZnSO}_4 \cdot 7\text{H}_2\text{O}$), 0.2 mg L^{-1} Nickel(II) chloride hexahydrate ($\text{NiCl}_2 \cdot 6\text{H}_2\text{O}$), 0.2 mg L^{-1} Copper (II) chloride dihydrate ($\text{CuCl}_2 \cdot 2\text{H}_2\text{O}$), 0.2 mg L^{-1} Sodium selenite pentahydrate ($\text{Na}_2\text{SeO}_3 \cdot 5\text{H}_2\text{O}$), 0.2 mg L^{-1} Sodium tungstate dihydrate ($\text{Na}_2\text{WO}_4 \cdot 2\text{H}_2\text{O}$). (a) Carbon dioxide transfer rate (CTR) [$\text{mmol L}^{-1} \text{h}^{-1}$]. (b) Total carbon dioxide (CT) [mmol L^{-1}] calculated as integral from the online CTR measurement. Cultivation conditions: Temperature: $T = 37^\circ\text{C}$, $\text{pH}_{t0} = 6$, shaking frequency: $n = 100 \text{ min}^{-1}$, shaking diameter: $d_o = 50 \text{ mm}$, culture volume: $V_L = 50 \text{ ml}$, absolute gas flow rate: $5 \text{ ml min}^{-1} \text{ N}_2$, medium = YTF medium, initial fructose concentration $c_{t0} = 5 \text{ g L}^{-1}$, inoculation density: $\text{OD}_{t0} = 0.1$, inoculation from actively growing pre-culture in serum bottle.

indicating less efficient carbon utilization. With added cobalt(II), the CTR curve was significantly influenced, but cultures displayed a similar CT to the reference without added trace elements. Even though the CTR curve with added nickel(II) had a similar progression as the control, a 15% decrease in CT was observed in comparison to the reference (Figure 3b). This increase in carbon utilization in the presence of nickel(II) might be explained by higher CODH/ACS activity without nickel(II) limitation.

The recorded CTR curves clearly show that iron(II) addition led to an unlimited exponential increase of metabolic activity. The logarithmic plot is shown in Figure S5. The addition of cobalt(II) initially led to linear increase of metabolic activity, while for the last 3 h of the cultivation (23–26 h), a steep vertical drop in CTR was observed. To obtain more detailed results on the influence of these metals on WLP activity in *C. ljungdahlii*, the addition of iron(II), cobalt(II), and nickel(II) was further investigated.

3.2 | Influence of iron(II)

The first trace metal investigated was iron(II). Some of the data was previously shown in Reference [54]. To obtain information on the effects of different concentrations, YTF medium was supplemented with 0, 2, 4, or 8 mg L⁻¹ of (NH₄)₂Fe(SO₄)₂·6H₂O. For growth phase I, as defined in Figure 2a, there was no observed difference in the CTR curves, independent of the amount of iron(II) added (Figure 4a). During phase II, the addition of increasing iron(II) concentrations prolonged the duration of exponential increase of the metabolic activity and led to higher maximum CTR values (Figure 4a). The addition of 8 mg L⁻¹ (NH₄)₂Fe(SO₄)₂·6H₂O prolonged exponential increase of the CTR by 10 h and resulted in exponential growth until fructose depletion (Figure 4a). The maximum CTR increased from 1.6 mmol L⁻¹ h⁻¹ to approximately 7.5 mmol L⁻¹ h⁻¹. Possibly, more available iron(II) leads to an enhanced ferredoxin maturation. Ferredoxin is required for various reactions catalyzed by *C. ljungdahlii* in both glycolysis and WLP, as discussed in the introduction. The observed CT was also slightly higher (13%) in the presence of higher concentrations of iron(II) (Figure 4b). The increase of the metabolic activity with increased iron(II) concentrations led to higher CO₂ production and higher CO₂ concentrations in the gas phase. In turn, this resulted in a net carbon loss in the cultivation since more CO₂ was removed via active ventilation during CTR measurement (Figure 1).

Besides increasing CO₂ production, iron(II) addition led to a slight shift in the product spectrum. With an increasing concentration of iron(II), titers of the more reduced product ethanol increased at the expense of acetate formation (Figure 4c). This result was expected in light of the increased CO₂ production observed during cultivation. Since CO₂ was not reduced in the WLP but released into the gas phase in the presence of increased iron(II) concentrations, acetate had to be reduced to ethanol to recycle electron carriers reduced during glycolysis. The shift toward ethanol in the presence of higher iron(II) concentrations occurs most probably since *C. ljungdahlii* converts acetate into ethanol using iron(II)-dependent alcohol dehydrogenase (Figure 1).¹³ Since the authors are not aware of a study reporting H₂ evolution from sugars by *C. ljungdahlii*, and the H₂ evolution from sugars reported for other acetogens is negligible as discussed before,²⁶ potential H₂ production is not considered in this study. In total, more biomass was produced with increased iron(II) availability (Figure 4c). This finding correlates well with the non-inhibited exponential CTR increase (Figure 4a). These results also correspond well to the findings of our previous study, where iron(II) was reported to

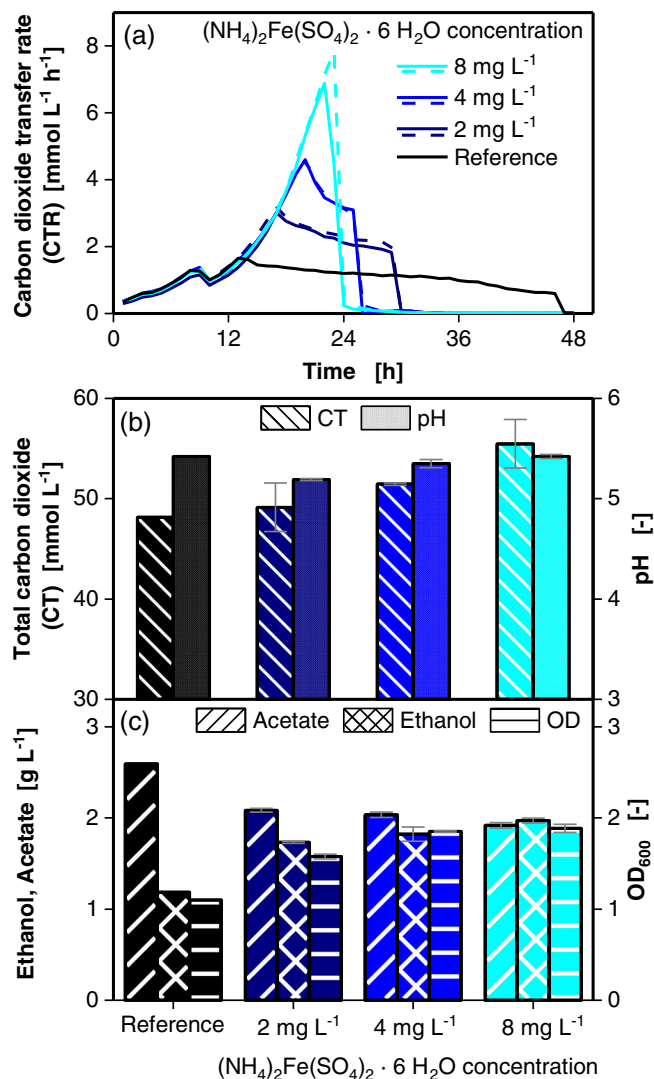


FIGURE 4 Influence of iron(II) in batch cultivation of *C. ljungdahlii* (DSM 13528) on fructose in seven 250 ml anaRAMOS flasks (Some of the data is taken from Reference [49]). Ammonium iron(II) sulphate hexahydrate ((NH₄)₂Fe(SO₄)₂·6H₂O) concentration is varied (0, 2, 4 and 8 mg L⁻¹). Duplicates are indicated by dashed lines. (a) Carbon dioxide transfer rate (CTR) (mmol L⁻¹ h⁻¹). (b) Total carbon dioxide (CT) (mmol L⁻¹) calculated as integral from the online CTR measurement and pH [-]. (c) Ethanol and acetate concentration (g L⁻¹) and OD₆₀₀ [-] determined at the end of the cultivation. Error bars indicate minimal and maximal value. Cultivation conditions: Temperature: $T = 37^{\circ}\text{C}$, $\text{pH}_{\text{t}0} = 6$, shaking frequency: $n = 100 \text{ min}^{-1}$, shaking diameter: $d_o = 50 \text{ mm}$, culture volume: $V_L = 50 \text{ ml}$, absolute gas flow rate: $5 \text{ ml min}^{-1} \text{ N}_2$, medium = YTF medium, initial fructose concentration $c_{\text{t}0} = 5 \text{ g L}^{-1}$, inoculation density: $\text{OD}_{\text{t}0} = 0.1$. Parts of the information were previously shown in reference 54.

display a positive influence on the alcohol production in *C. carboxidivorans*.⁴²

Carbon balances were calculated with CT data and measured product titers (Figure S6). With increasing iron(II) concentrations, total carbon in CO₂ and products slightly increased. Carbon balances were calculated for all experiments and revealed slightly higher amounts of

carbon in the products than supplemented via fructose in the presence of added iron(II) (Figures S6–S8). This hints at an improved utilization of complex substrates like yeast extract in the presence of added iron(II).

3.3 | Influence of cobalt(II)

The second trace element investigated in detail was cobalt(II). *C. ljungdahlii* was cultivated in the presence of either 0, 1, 2, or 4 mg L⁻¹ of added CoCl₂·6H₂O (Figure 5). In the first 12 h of cultivation, no difference in growth behavior was observed, independent of the added cobalt(II) concentration. After the second CTR peak after 12 h, a linear increase of the CTR was observed in cultures with added cobalt(II), but not in the reference. Without added cobalt(II), the CTR curve followed the same pattern as in previous experiments, where measured CTR slowly declined over time. In the presence of added cobalt(II), the CTR decreased sharply after 23 h before fructose depleted after 26 h, and no more CO₂ production was observed. The first peak, indicating depletion of complex growth substrates, was similar in all cultivations. Curiously, a small additional peak appeared in cultivations with added cobalt(II), precisely at the same time as peak II occurred in the reference cultivation (indicated by an arrow in Figure 5). Since we did not observe this peak when iron(II) was added to cultivations (compare Figure 4), we conclude that this local maximum in CTR indicated the onset of iron(II) limitation in cultures with added cobalt(II). Potentially, this could be an indicator that cobalt(II) can partly replace iron(II).

The cultivation duration with added cobalt(II) was decreased by approximately 12 h, compared to the reference cultivation in YTF medium without added cobalt(II). Even though the addition of 1 mg L⁻¹ cobalt(II) had a dramatic effect on CTR compared to the control, higher concentrations only led to slightly increasing CTR values. CT values were similar in all cultivations, independent of the added cobalt(II) concentration (Figure 5b). More biomass was formed in the presence of additional cobalt(II). Ethanol titers increased slightly at the expense of acetate, causing a higher final pH due to decreased acid production (Figure 5b,c). Much like CTR values, the effect was not influenced by higher cobalt(II) concentrations. Calculation of carbon balances confirmed that all carbon derived from fructose was metabolized into either CO₂, biomass, acetate, or ethanol (Figure S7). These results show that the addition of cobalt(II) strongly influences CTR progression, growth, and product formation of *C. ljungdahlii*, but above 1 mg L⁻¹ added cobalt(II) no concentration effect was observed.

3.4 | Influence of nickel(II) and iron(II)

The third trace element investigated in more detail was nickel(II). *C. ljungdahlii* was cultivated in the presence of either 0, 0.1, 0.2 or 0.4 mg L⁻¹ of NiCl₂·6H₂O. Since previous results clearly showed a secondary substrate limitation from insufficient iron(II) (see Figure 3),

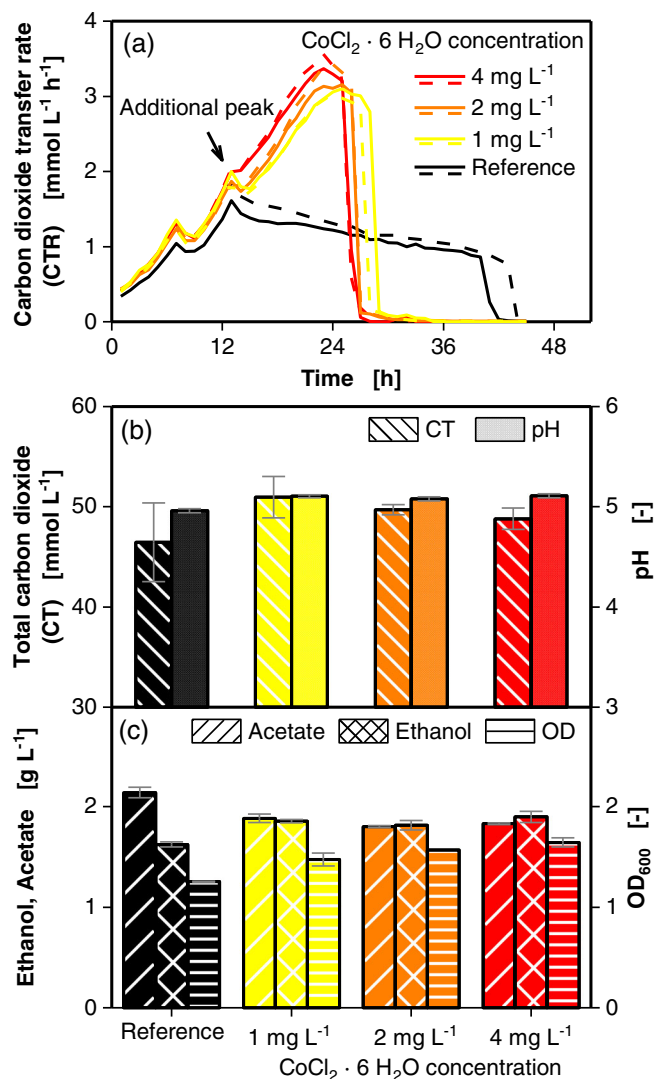


FIGURE 5 Influence of cobalt(II) in batch cultivation of *C. ljungdahlii* (DSM 13528) on fructose in eight 250 ml anaRAMOS flasks. Cobalt(II) chloride hexahydrate (CoCl₂·6H₂O) concentration is set to 0, 1, 2 and 4 mg L⁻¹. Each condition was tested in duplicate (dashed lines). (a) Carbon dioxide transfer rate (CTR) (mmol L⁻¹ h⁻¹). (b) Total carbon dioxide (CT) (mmol L⁻¹) calculated as integral from the online CTR measurement and pH [-]. (c) Ethanol and acetate concentration (g L⁻¹) and OD₆₀₀ [-] determined at the end of the cultivation. Error bars indicate minimal and maximal value. Cultivation conditions: Temperature: $T = 37^{\circ}\text{C}$, $\text{pH}_{\text{t}0} = 6$, shaking frequency: $n = 100 \text{ min}^{-1}$, shaking diameter: $d_{\text{O}} = 50 \text{ mm}$, culture volume: $V_{\text{L}} = 50 \text{ ml}$, absolute gas flow rate: $5 \text{ ml min}^{-1} \text{ N}_2$, medium = YTF medium, initial fructose concentration $c_{\text{t}0} = 5 \text{ g L}^{-1}$, inoculation density: $\text{OD}_{\text{t}0} = 0.1$.

an additional 8 mg L⁻¹ of (NH₄)₂Fe(SO₄)₂·6H₂O were supplemented to all cultivations in this experiment. We observed no influence of added nickel(II) on fermentation phase I, as defined in Figure 2 (Figure 6). However, the maximum CTR decreased with higher nickel(II) concentrations and occurred earlier compared to the reference. While the maximum CTR of the reference cultivation was 6.4 mmol L⁻¹ h⁻¹, the addition of 0.4 mg L⁻¹ NiCl₂·6H₂O decreased the maximum CTR by 42% to 3.7 mmol L⁻¹ h⁻¹. While in the

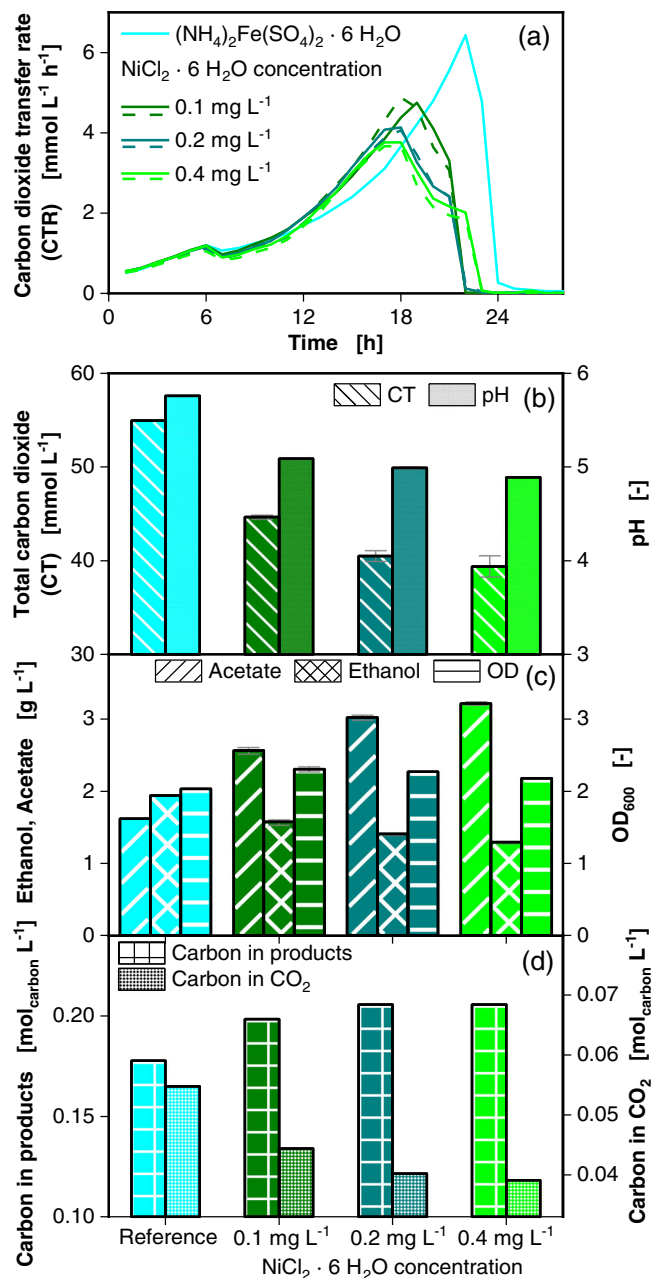


FIGURE 6 Influence of nickel(II) on batch cultivation of *C. ljungdahliae* (DSM 13528) on fructose in seven 250 ml anaRAMOS flasks in YTF medium with 8 mg L^{-1} Ammonium iron(II) sulphate hexahydrate $(\text{NH}_4)_2\text{Fe}(\text{SO}_4)_2 \cdot 6\text{H}_2\text{O}$. Varying concentrations of Nickel(II) chloride hexahydrate ($\text{NiCl}_2 \cdot 6\text{H}_2\text{O}$) were added (0.1, 0.2 and 0.4 mg L^{-1}), duplicates are indicated by dashed lines. (a) Carbon dioxide transfer rate (CTR) ($\text{mmol L}^{-1} \text{h}^{-1}$). (b) Total carbon dioxide (CT) (mmol L^{-1}) calculated as integral from the online CTR measurement and pH [-]. (c) Ethanol and acetate concentration (g L^{-1}) and OD_{600} [-] determined at the end of the cultivation. Error bars indicate minimal and maximal value. (d) Carbon in products and carbon in CO_2 at the end of the cultivation. Cultivation conditions: Temperature: $T = 37^\circ\text{C}$, $\text{pH}_{t0} = 6$, shaking frequency: $n = 100 \text{ min}^{-1}$, shaking diameter: $d_0 = 50 \text{ mm}$, culture volume: $V_L = 50 \text{ ml}$, absolute gas flow rate: $5 \text{ ml min}^{-1} \text{ N}_2$, medium = YTF medium, initial fructose concentration $c_{t0} = 5 \text{ g L}^{-1}$, inoculation density: $\text{OD}_{t0} = 0.1$.

reference cultivation, the CTR dropped to $0 \text{ mmol L}^{-1} \text{h}^{-1}$ directly after the maximum was reached. CTR curves in the presence of nickel(II) sloped down more gently, after reaching their maximum values (Figure 6a).

Compared to the reference, CO_2 production (CT) decreased by 28% in cultures with added 0.4 mg L^{-1} of $\text{NiCl}_2 \cdot 6\text{H}_2\text{O}$ (Figure 6b), indicating higher WLP activity if nickel(II) is available. Since the crucial enzyme in the WLP, the CODH/ACS responsible for the formation of acetyl-CoA, is strictly nickel(II) dependent.³⁷ It can be assumed, that an increased nickel(II) availability results in an increased CODH/ACS activity and thus higher CO_2 reassimilation. Higher nickel(II) availability also led to an increase in acetate production at the expense of ethanol production and correlated to a downward shift in final pH (Figure 6b,c). The higher carbon utilization efficiency is explained by increased WLP activity. Since more electrons are diverted toward CO_2 reduction to acetate, fewer electrons are available to reduce acetate to ethanol.⁵⁵ This causes a higher ratio of soluble products (acetate and ethanol) to CO_2 with higher nickel(II) availability (Figure 6d). Biomass yields also increased with added nickel(II) compared to the reference cultivation, but there was no correlation between higher nickel(II) concentrations and biomass yields. Total product carbon balances were calculated and showed a slight increase in carbon metabolized into products (CO_2 , acetate, and ethanol) in the presence of added nickel(II) (Figure S8). In conclusion, $\text{NiCl}_2 \cdot 6\text{H}_2\text{O}$ (and Fe(II)) addition to complex medium resulted in higher growth yield. It increased acetate formation at the expense of ethanol and CO_2 formation, indicating higher WLP activity, most probably due to alleviated limitation of CODH/ACS.

To gain further information on the influence of nickel(II) availability on the growth and production behavior of *C. ljungdahliae*, additional cultivations were performed, and offline sampled to generate data for OD and products. The results were correlated with the CTR curves recorded by the anaRAMOS (Figure 7). When only Fe(II) (8 mg L^{-1} of $(\text{NH}_4)_2\text{Fe}(\text{SO}_4)_2 \cdot 6\text{H}_2\text{O}$) was added, cells displayed a diauxic growth behavior with higher initial exponential growth for the first 8–10 h, followed by a second, slower exponential growth rate (indicated by log OD in Figure 7b,e). The same applies for online measured CTR (indicated by log CTR in Figure 7b,e). This was accompanied by a first CTR peak at 6 h and a subsequent short decline in CTR before it rose again to a second, much higher peak after approximately 22 h and a sharp decline toward 0 net CO_2 evolution (Figure 7a). However, if Ni(II) (0.4 mg L^{-1} $\text{NiCl}_2 \cdot 6\text{H}_2\text{O}$) and Fe(II) (8 mg L^{-1} of $(\text{NH}_4)_2\text{Fe}(\text{SO}_4)_2 \cdot 6\text{H}_2\text{O}$) were added together, no strict diauxic growth behavior was observed in the OD measurements. The CTR sloped off earlier and more gently after 17 h of growth (Figure 7d). These results highlight the importance of online CTR monitoring, as sole monitoring of the OD would not have provided the distinct difference between growth (OD) and metabolic activity (CTR). Likely, the change in the metabolic activity results from more efficient carbon utilization, resulting in a reduced CT, as shown in Figure 6.

During the first 6–8 h of cultivation, acetate formation was similar at both conditions tested. While in the presence of only added iron(II), no alcohol formation was observed, added nickel(II) also facilitated

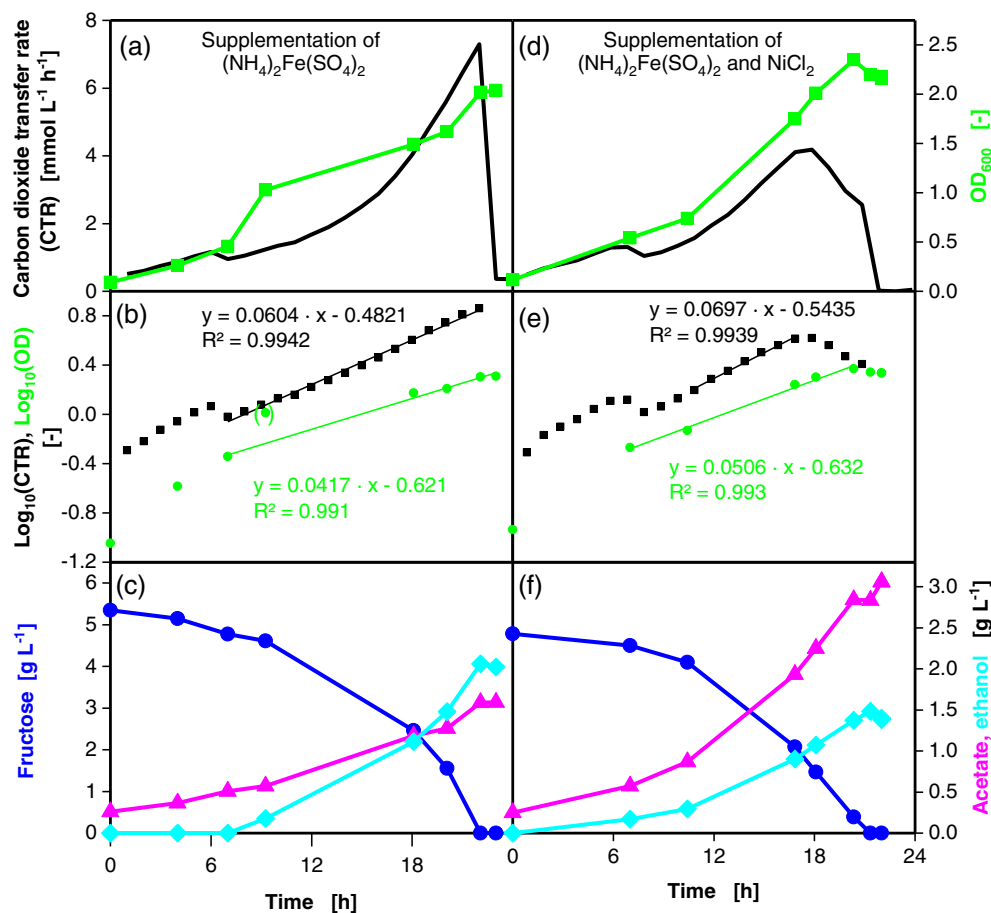


FIGURE 7 Comparison of iron(II) or iron(II) + nickel(II) supplementation on batch cultivation of *C. ljungdahlii* (DSM 13528) on fructose in YTF medium (Some of the data is taken from Reference [49]). For each sampling point, one flask was removed and not further used for online monitoring. (a and d) Carbon dioxide transfer rate (CTR) [mmol L⁻¹ h⁻¹] and optical density (OD₆₀₀) [–]. (b and e) Logarithmic plot of the carbon dioxide transfer rate (Log₁₀(CTR)) and logarithmic plot of the optical density (Log₁₀(OD)). (c and f) Fructose, ethanol and acetate concentration (g L⁻¹) over time. Cultivation conditions: Temperature: $T = 37^\circ\text{C}$, $\text{pH}_{t0} = 6$, shaking frequency: $n = 100 \text{ min}^{-1}$, shaking diameter: $d_o = 50 \text{ mm}$, culture volume: $V_L = 50 \text{ ml}$, absolute gas flow rate: $5 \text{ ml min}^{-1} \text{ N}_2$, medium = YTF medium, initial fructose concentration $c_{t0} = 5 \text{ g L}^{-1}$, inoculation density: $\text{OD}_{t0} = 0.1$.

ethanol production at this early stage. After 8 h, however, there was a steep increase in ethanol production in the cultivation with only added iron(II), leading to 2 g L^{-1} ethanol and 1.5 g L^{-1} acetate at the end of cultivation (Figure 7c). With added Ni(II), final titers of 1.5 g L^{-1} ethanol and 3 g L^{-1} acetate were produced (Figure 7f). After 20 to 22 h, fructose was depleted at both conditions tested. The offline measured depletion of fructose goes well in hand with the online detected halt of the metabolic activity, indicated by the abrupt drop of the CTR. This phenomenon is caused by the generally low K_M values of microorganisms for preferred carbon sources like fructose. In conclusion, even though growth rates and CT were lower in the presence of added nickel(II), final biomass and product yields were strongly increased compared to the reference. This indicates much higher carbon utilization efficiency if nickel(II) is available during growth in complex medium.

The logarithmic plot of the CTR and the OD (Figure 7b,e) supports the observations discussed for Figure 7a,d. When only iron(II) is added, both the CTR and the OD show exponential increase throughout the second cultivation phase (Figure 7b). When iron(II) and nickel(II) are added, the exponential increase in CTR ceases before fructose depletion (Figure 7e). In contrast, the logarithmic plot of the OD shows an exponential increase until fructose depletion (Figure 7e). These results clearly indicate, that online measurement with the anaRAMOS device provides valuable insights into metabolic activity, which can otherwise not be deduced solely by offline sampling.

3.5 | Influence of volumetric ventilation rate on the CO₂ utilization

The results of the previous experiments clearly show a relation between the metabolic activity of *C. ljungdahlii* on fructose and the availability of CO₂ as an electron acceptor. Given that the volume of the culture vessel and the absolute flow rate of gas remains constant, an increased filling volume results in a decreased volumetric ventilation rate and thus less CO₂ stripping. Hence, cultivations with iron(II) and nickel(II) were conducted using different filling volumes, in order to investigate the influence of the volumetric ventilation rate in the cultivation vessel. Cultivations with either 10, 50, or 80 ml medium (resulting in a volumetric ventilation rates of 0.5, 0.1 and 0.063 min^{-1} , respectively) in 250 ml RAMOS flasks were performed (Figure 8). The progressions of the CTR over time for 50 and 80 ml filling volumes were similar to the ones in previous experiments, which were performed with 50 ml medium in the same flasks. However, the cultivation with 10 ml filling volume showed a lower growth rate after 12 h cultivation time, leading to a delayed second CTR peak at 22 h compared to 16 h with larger filling volumes. Furthermore, a steeper decline in CTR was observed after the second peak in the cultivation with 10 ml medium.

The CT for the 10 ml cultures (39 mmol L^{-1}) was 13 mmol L^{-1} higher than values for the 50 and 80 ml cultures (both 52 mmol L^{-1}). In total, this accounts for a reduction of carbon loss by 25% at larger

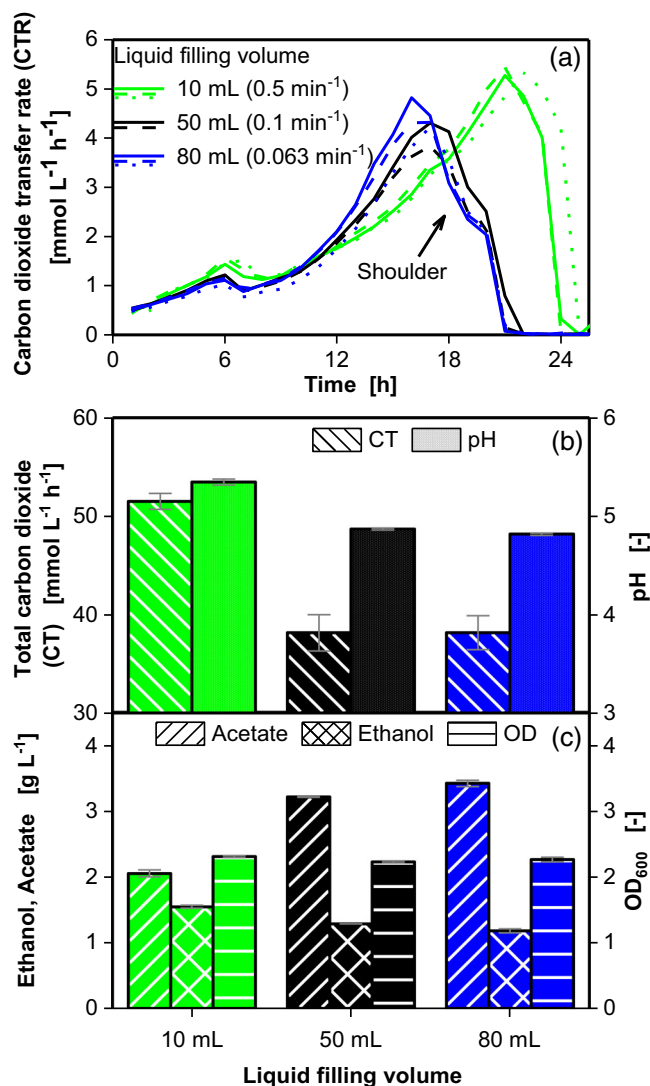


FIGURE 8 Influence of liquid filling volume on cultivation of *C. ljungdahliae* (DSM 13528) on fructose in eight 250 ml anaRAMOS flasks using YTF medium containing 8 mg L^{-1} Ammonium iron(II) sulphate hexahydrate ($(\text{NH}_4)_2\text{Fe}(\text{SO}_4)_2 \cdot 6\text{H}_2\text{O}$) and 0.4 mg L^{-1} of Nickel(II) chloride hexahydrate ($\text{NiCl}_2 \cdot 6\text{H}_2\text{O}$). Filling volumes varied between 10 and 80 ml. Duplicates and triplicates are indicated by dashed and dotted lines. Each flask was ventilated using 5 ml min^{-1} of N_2 , resulting in volumetric ventilation rates of 0.5, 0.1 and 0.063 min^{-1} . (a) Carbon dioxide transfer rate (CTR) ($\text{mmol L}^{-1} \text{h}^{-1}$). (b) Total carbon dioxide (CT) (mmol L^{-1}) calculated as integral from the online CTR measurement and pH [–]. (c) Ethanol and acetate concentration (g L^{-1}) and OD_{600} [–] determined at the end of the cultivation. Error bars indicate minimal and maximal value. Cultivation conditions: Temperature: $T = 37^\circ\text{C}$, $\text{pH}_{t0} = 6$, shaking frequency: $n = 100 \text{ min}^{-1}$, shaking diameter: $d_o = 50 \text{ mm}$, culture volume: $V_L = 10\text{--}80 \text{ ml}$, absolute gas flow rate: $5 \text{ ml min}^{-1} \text{ N}_2$, medium = YTF medium, initial fructose concentration $c_{t0} = 5 \text{ g L}^{-1}$, inoculation density: $\text{OD}_{t0} = 0.1$.

filling volumes. This was to be expected since higher availability of dissolved CO_2 in the larger media volumes allows the cells to form more acetate in the WLP and simultaneously decreases the need to recycle reducing equivalents via acetate reduction to ethanol. In accordance

with the higher acetate-ethanol ratio (Figure 8c), the pH value decreased with larger filling volumes (Figure 8b). The results in the experiment with increased filling volume was similar to the results for increasing nickel(II) concentrations. Both, a larger filling volume (Figure 8b) and a higher nickel(II) concentration (with iron(II) present) (Figure 6b), allow for an enhanced CO_2 utilization via the WLP and shift the product spectrum toward acetate production. Interestingly, an increase in filling volume in standard YTF medium without the addition of iron(II) and nickel(II) displayed the same trend (Figure S5). Even though WLP activity was limited due to a shortage of trace metals, increased availability of dissolved CO_2 (higher filling volume) led to shorter cultivation times and reduced CO_2 release. However, this effect was less pronounced than in the presence of added iron(II) and nickel(II).

Carbon fixation via the WLP is enhanced by increased iron(II) and nickel(II) concentrations and higher CO_2 partial pressures. Increasing activity of the WLP in both cases (Figures 6 and 8) leads to faster growth and a decreased carbon loss in the form of CO_2 into the gas phase.

4 | CONCLUSION

In this study, the anaRAMOS was applied for online CTR measurement for the investigation of *C. ljungdahliae*'s metabolic response, when grown in YTF medium with added trace elements (TE). The online measurement of evolved CO_2 allowed for a relative evaluation of WLP activity during glycolysis in different environments (TE availability and CO_2 stripping rates). These online data can be used to evaluate the impact of TE on different metabolic modules (glycolysis, WLP and reduction of acetate to ethanol) as well as display the exact time point during the fermentation when inhibition occurs. These observations are only possible with online measurement of the CTR as a direct metabolic marker for metabolic activity, clearly underlining the importance and possibilities of applying real-time analysis with the anaRAMOS. Additionally, it is demonstrated that the utilization of online monitoring devices drastically reduces the need to take offline samples. With these results we were able to show, that the model acetogen *C. ljungdahliae* displays only background WLP activity during heterotrophic growth in YTF medium, even though WLP activity would lead to higher acetyl-CoA availability and ATP yields. This lack in WLP activity is caused by TE limitation. To avoid TE limitations when cultivating acetogenic bacteria in complex media, a TE composition, optimized for the strain in question, should be added to complex media. The composition of the TE has to be adjusted depending on the goal of the respective cultivation.

For *C. ljungdahliae* cultivations in YTF medium, iron(II), cobalt(II), and nickel(II) were identified to influence the CO_2 production, the product spectrum, and biomass formation. The addition of iron(II) led to increased ethanol production. The addition of nickel(II) and iron(II) led to a reduction of CO_2 production by 28%. In comparison, an increase of the filling volume resulted in a reduction of CO_2 emission by 25%. In both cases, the product spectrum was shifted toward acetate, indicating more efficient carbon utilization during recycling of

NADH and ferredoxin reduced during glycolysis. The reported results help to better understand the metabolic activity of *C. ljungdahlii* and the influence of trace elements on product and biomass formation. With this study as a proof of concept, it is now feasible to evaluate different media compositions, growth substrates and cultivation conditions for acetogenic bacteria, to characterize their behavior and improve strains and fermentation conditions. In the next steps, a more detailed analyses concerning the influence of additionally supplemented CO₂ on heterotrophic growth needs to be conducted. Future experiments could also investigate other carbon sources. The RAMOS device was recently adjusted to syngas as carbon source.⁵⁶

ACKNOWLEDGMENTS

We would like to thank BMBF for funding this project (03INT513BE) and the European Union for funding this project (Agreement No. 761042).

CONFLICT OF INTEREST

The authors declare no conflict of interest.

AUTHOR CONTRIBUTIONS

Marcel Mann designed the study, conducted the experiments, analyzed and interpreted data, and drafted the manuscript. Darina Effert conducted experiments and analyzed data. Patrick Kottenhahn interpreted data and drafted the manuscript. Aline Hüser supported with analyzing data. Gabriele Philipps interpreted data and supported drafting the manuscript. Stefan Jennewein interpreted data and critically revised the manuscript. Jochen Büchs initiated and supervised the study, participated in data interpretation, drafting the manuscript, and critically revised the manuscript.

DATA AVAILABILITY STATEMENT

All data is available on request to the corresponding author.

ORCID

Marcel Mann  <https://orcid.org/0000-0002-2819-0358>

REFERENCES

- European Commission. 2030 Climate & Energy Framework. https://ec.europa.eu/clima/policies/strategies/2030_en. Accessed March 5, 2020.
- European Commission. 2050 Long-Term Strategy; 2020. https://ec.europa.eu/clima/policies/strategies/2050_en.
- Hu P, Chakraborty S, Kumar A, et al. Integrated bioprocess for conversion of gaseous substrates to liquids. *Proc Natl Acad Sci*. 2016; 113(14):3773-3778. doi:10.1073/pnas.1516867113
- Griffin DW, Schultz MA. Fuel and chemical products from biomass syngas: a comparison of gas fermentation to thermochemical conversion routes. *Environ Prog Sustain Energy*. 2012;31(2):219-224. doi:10.1002/ep.11613
- Daniell J, Köpke M, Simpson S. Commercial biomass syngas fermentation. *Energies*. 2012;5(12):5372-5417. doi:10.3390/en5125372
- De Tissera S, Köpke M, Simpson SD, Humphreys C, Minton NP, Dürre P. Syngas biorefinery and syngas utilization. In: Wagemann K, Tippkötter N, eds. *Biorefineries*. Springer International Publishing; 2017:247-280. doi:10.1007/10_2017_5
- Fernández-Naveira Á, Abubackar HN, Veiga MC, Kennes C. Production of chemicals from C1 gases (CO, CO₂) by clostridium carboxidivorans. *World J Microbiol Biotechnol*. 2017;33(3):43. doi:10.1007/s11274-016-2188-z
- Liew F, Martin ME, Tappel RC, Heijstra BD, Mihalcea C, Köpke M. Gas fermentation—a flexible platform for commercial scale production of low-carbon-fuels and chemicals from waste and renewable feedstocks. *Front Microbiol*. 2016;7:694. doi:10.3389/fmicb.2016.00694
- Cheng C, Bao T, Yang S-T. Engineering clostridium for improved solvent production: recent progress and perspective. *Appl Microbiol Biotechnol*. 2019;103(14):5549-5566. doi:10.1007/s00253-019-09916-7
- Dürre P. Biobutanol: An attractive biofuel. *Biotechnol J*. 2007;2(12):1525-1534. doi:10.1002/biot.200700168
- Diender M, Stams AJM, Sousa DZ. Production of medium-chain fatty acids and higher alcohols by a synthetic co-culture grown on carbon monoxide or syngas. *Biotechnol Biofuels*. 2016;9(1):82-93. doi:10.1186/s13068-016-0495-0
- Müller V. Energy conservation in acetogenic bacteria. *Appl Environ Microbiol*. 2003;69(11):6345-6353. doi:10.1128/AEM.69.11.6345-6353.2003
- Köpke M, Held C, Hujer S, et al. *Clostridium ljungdahlii* represents a microbial production platform based on syngas. *Proc Natl Acad Sci*. 2010;107(29):13087-13092. doi:10.1073/pnas.1004716107
- Schuchmann K, Müller V. Autotrophy at the thermodynamic limit of life: a model for energy conservation in acetogenic bacteria. *Nat Rev Microbiol*. 2014;12(12):809-821. doi:10.1038/nrmicro3365
- Drake HL, Gößner AS, Daniel SL. Old acetogens, new light. *Ann N Y Acad Sci*. 2008;1125(1):100-128. doi:10.1196/annals.1419.016
- Fontaine FE, Peterson WH, McCoy E, Johnson MJ, Ritter GJ. A new type of glucose fermentation by *Clostridium thermoaceticum*. *J Bacteriol*. 1942;43(6):701-715. <https://pubmed.ncbi.nlm.nih.gov/16560531>
- Schuchmann K, Müller V. Energetics and application of heterotrophy in Acetogenic bacteria. Stams AJM, ed. *Appl Environ Microbiol*. 2016; 82(14):4056-4069. doi:10.1128/AEM.00882-16
- Mueller V. Bacterial fermentation. *Encyclopedia of Life Sciences*. Chichester, UK; 2008. doi:10.1002/9780470015902.a0001415.pub2
- Schoelmerich MC, Katsyov A, Sung W, et al. Regulation of lactate metabolism in the acetogenic bacterium *Acetobacterium woodii*. *Environ Microbiol*. 2018;20(12):4587-4595. doi:10.1111/1462-2920.14412
- Bertsch J, Siemund AL, Kremp F, Müller V. A novel route for ethanol oxidation in the acetogenic bacterium *Acetobacterium woodii*: the acetaldehyde/ethanol dehydrogenase pathway. *Environ Microbiol*. 2016;18(9):2913-2922. doi:10.1111/1462-2920.13082
- Keller A, Schink B, Müller N. Alternative pathways of acetogenic ethanol and methanol degradation in the thermophilic anaerobe *Thermacetogenium phaeum*. *Front Microbiol*. 2019;10. doi:10.3389/fmicb.2019.00423
- Buschhorn H, Dürre P, Gottschalk G. Production and utilization of ethanol by the Homoacetogen *Acetobacterium woodii*. *Appl Environ Microbiol*. 1989;55(7):1835-1840. doi:10.1128/aem.55.7.1835-1840.1989
- Valgepea K, de Souza Pinto Lemgruber R, Meaghan K, et al. Maintenance of ATP homeostasis triggers metabolic shifts in gas-fermenting acetogens. *Cell Syst*. 2017;4(5):505-515. doi:10.1016/j.cels.2017.04.008
- Tan Y, Liu J, Chen X, Zheng H, Li F. RNA-seq-based comparative transcriptome analysis of the syngas-utilizing bacterium *Clostridium ljungdahlii* DSM 13528 grown autotrophically and heterotrophically. *Mol Biosyst*. 2013;9(11):2775-2784. doi:10.1039/c3mb70232d
- Huang H, Wang S, Moll J, Thauer RK. Electron bifurcation involved in the energy metabolism of the acetogenic bacterium *Moorella thermoacetica* growing on glucose or H₂ plus CO₂. *J Bacteriol*. 2012;194(14):3689-3699. doi:10.1128/JB.00385-12

26. Kellum R, Drake HL. Effects of cultivation gas phase on hydrogenase of the acetogen *Clostridium thermoaceticum*. *J Bacteriol*. 1984;160(1):466-469. doi:10.1128/jb.160.1.466-469.1984
27. Lee S-H, Yun EJ, Kim J, Lee SJ, Um Y, Kim KH. Biomass, strain engineering, and fermentation processes for butanol production by solventogenic clostridia. *Appl Microbiol Biotechnol*. 2016;100(19):8255-8271. doi:10.1007/s00253-016-7760-9
28. Ramió-Pujol S, Ganigué R, Bañeras L, Colprim J. Effect of ethanol and butanol on autotrophic growth of model homoacetogens. *FEMS Microbiol Lett*. 2018;365(10):10-13. doi:10.1093/femsle/fny084
29. Whitham JM, Schulte MJ, Bobay BG, et al. Characterization of *Clostridium ljungdahlii* OTA1: a non-autotrophic hyper ethanol-producing strain. *Appl Microbiol Biotechnol*. 2017;101(4):1615-1630. doi:10.1007/s00253-016-7978-6
30. Köpke M, Mihalcea C, Bromley JC, Simpson SD. Fermentative production of ethanol from carbon monoxide. *Curr Opin Biotechnol*. 2011;22(3):320-325. doi:10.1016/j.copbio.2011.01.005
31. Saxena J, Tanner RS. Effect of trace metals on ethanol production from synthesis gas by the ethanologenic acetogen, *Clostridium ragsdalei*. *J Ind Microbiol Biotechnol*. 2011;38(4):513-521. doi:10.1007/s10295-010-0794-6
32. Richter H, Martin M, Angenent L. A two-stage continuous fermentation system for conversion of syngas into ethanol. *Energies*. 2013;6(8):3987-4000. doi:10.3390/en6083987
33. Richter H, Molitor B, Diender M, Sousa DZ, Angenent LT. A narrow pH range supports butanol, hexanol, and octanol production from syngas in a continuous co-culture of *Clostridium ljungdahlii* and *Clostridium kluyveri* with in-line product extraction. *Front Microbiol*. 2016;11(55). doi:10.3389/fmicb.2016.01773
34. Zhao R, Liu Y, Zhang H, et al. CRISPR-Cas12a-mediated gene deletion and regulation in *Clostridium ljungdahlii* and its application in carbon flux redirection in synthesis gas fermentation. *ACS Synth Biol*. 2019;8(10):2270-2279. doi:10.1021/acssynbio.9b00033
35. Molitor B, Kirchner K, Henrich AW, Schmitz S, Rosenbaum MA. Expanding the molecular toolkit for the homoacetogen *Clostridium ljungdahlii*. *Sci Rep*. 2016;6(1). doi:10.1038/srep31518
36. Philipps G, de Vries S, Jennewein S. Development of a metabolic pathway transfer and genomic integration system for the syngas-fermenting bacterium *Clostridium ljungdahlii*. *Biotechnol Biofuels*. 2019;12(1):1-12. doi:10.1186/s13068-019-1448-1
37. Ragsdale SW. Enzymology of the Wood-Ljungdahl pathway of acetogenesis. *Ann N Y Acad Sci*. 2008;1125(1):129-136. doi:10.1196/annals.1419.015
38. Phillips JR, Atiyeh HK, Tanner RS, et al. Butanol and hexanol production in *Clostridium carboxidivorans* syngas fermentation: medium development and culture techniques. *Bioresour Technol*. 2015;190:114-121. doi:10.1016/j.biortech.2015.04.043
39. Buchanan BB, Lovenberg W, Rabinowitz JC. A comparison of clostridial ferredoxins. *Proc Natl Acad Sci*. 1963;49(3):345-353. doi:10.1073/pnas.49.3.345
40. Blomstrom DC, Knight E, Phillips WD, Weiher JF. The nature of iron in ferredoxin. *Proc Natl Acad Sci*. 1964;51(6):1085-1092. doi:10.1073/pnas.51.6.1085
41. Bertsch J, Müller V. Bioenergetic constraints for conversion of syngas to biofuels in acetogenic bacteria. *Biotechnol Biofuels*. 2015;8(1):210. doi:10.1186/s13068-015-0393-x
42. Shen S, Gu Y, Chai C, Jiang W, Zhuang Y, Wang Y. Enhanced alcohol titre and ratio in carbon monoxide-rich off-gas fermentation of *Clostridium carboxidivorans* through combination of trace metals optimization with variable-temperature cultivation. *Bioresour Technol*. 2017;239:236-243. doi:10.1016/j.biortech.2017.04.099
43. Han Y-F, Xie B-T, Wu G, Guo Y-Q, Li D-M, Huang Z-Y. Combination of trace metal to improve solventogenesis of *Clostridium carboxidivorans* P7 in syngas fermentation. *Front Microbiol*. 2020;11. doi:10.3389/fmicb.2020.577266
44. Hu SI, Pezacka E, Wood HG. Acetate synthesis from carbon monoxide by *Clostridium thermoaceticum*. Purification of the corrinoid protein. *J Biol Chem*. 1984;259(14):8892-8897. <http://www.ncbi.nlm.nih.gov/pubmed/6746629>
45. Yang G, Hong S, Yang P, et al. Discovery of an ene-reductase for initiating flavone and flavonol catabolism in gut bacteria. *Nat Commun*. 2021;12(1):790. doi:10.1038/s41467-021-20974-2
46. Philips J, Rabaey K, Lovley DR, Vargas M. Biofilm formation by *Clostridium ljungdahlii* is induced by sodium chloride stress: experimental evaluation and transcriptome analysis. *PLoS One*. 2017;12(1):e0170406. doi:10.1371/journal.pone.0170406
47. Zhang C, Nie X, Zhang H, et al. Functional dissection and modulation of the BirA protein for improved autotrophic growth of gas-fermenting *Clostridium ljungdahlii*. *Microb Biotechnol*. 2021;14(5):2072-2089. doi:10.1111/1751-7915.13884
48. Liu Z-Y, Jia D-C, Zhang K-D, et al. Ethanol metabolism dynamics in *Clostridium ljungdahlii* grown on carbon monoxide. *Appl Environ Microbiol*. 2020;86(14):1-13. doi:10.1128/AEM.00730-20
49. Mann M, Wittke D, Büchs J. Online monitoring applying the anaerobic respiratory monitoring system reveals iron(II) limitation in YTF medium for *Clostridium ljungdahlii*. *Eng Life Sci*. 2020;elsc.202000054. doi:10.1002/elsc.202000054
50. Munch G, Schulte A, Mann M, et al. Online measurement of CO₂ and total gas production in parallel anaerobic shake flask cultivations. *Biochem Eng J*. 2019;153:1-8. doi:10.1016/j.bej.2019.107418
51. Leang C, Ueki T, Nevin KP, Lovley DR. A genetic system for *Clostridium ljungdahlii*: a chassis for autotrophic production of bio-commodities and a model Homoacetogen. *Appl Environ Microbiol*. 2013;79(4):1102-1109. doi:10.1128/AEM.02891-12
52. Atkinson B, Mavituna F. *Biochemical Engineering and Biotechnology Handbook*. [Contains Glossary]. Nature Press; 1982.
53. Anderlei T, Büchs J. Device for sterile online measurement of the oxygen transfer rate in shaking flasks. *Biochem Eng J*. 2001;7(2):157-162. doi:10.1016/S1369-703X(00)00116-9
54. Mann M, Wittke D, Büchs J. Online monitoring applying the anaerobic respiratory monitoring system reveals iron(II) limitation in YTF medium for *Clostridium ljungdahlii*. *Eng Life Sci*. 2021;21(1-2):19-28. doi:10.1002/elsc.202000054
55. Cheng C, Shao Y, Li W, et al. Electricity-enhanced anaerobic, non-photosynthetic mixotrophy by *Clostridium carboxidivorans* with increased carbon efficiency and alcohol production. *Energy Convers Manag*. 2022;252:115118. doi:10.1016/j.enconman.2021.115118
56. Mann M, Hüser A, Schick B, Dinger R, Miebach K, Büchs J. Online monitoring of gas transfer rates during CO and CO/H₂ gas fermentation in quasi-continuously ventilated shake flasks. *Biotechnol Bioeng*. 2021;118(5):2092-2104. doi:10.1002/bit.27722

SUPPORTING INFORMATION

Additional supporting information may be found in the online version of the article at the publisher's website.

How to cite this article: Mann M, Effert D, Kottenhahn P, et al. Impact of different trace elements on metabolic routes during heterotrophic growth of *C. ljungdahlii* investigated through online measurement of the carbon dioxide transfer rate. *Biotechnol. Prog.* 2022;e3263. doi:10.1002/btpr.3263